Plant Molecular Biology (2018) 97:113–130
https://doi.org/10.1007/s11103-018-0727-8

Developmental transcriptome analysis of floral transition in *Rosa odorata* var. *gigantea*

Xuelian Guo[1] · Chao Yu[1] · Le Luo[1] · Huihua Wan[1] · Ni Zhen[1] · Yushu Li[1] · Tangren Cheng[1] · Jia Wang[1] · Huitang Pan[1] · Qixiang Zhang[1,2]

Received: 6 December 2016 / Accepted: 3 April 2018 / Published online: 7 May 2018

Abstract

Key message **Expression analyses revealed that floral transition of *Rosa odorata* var. *gigantea* is mainly regulated by *VRN1, COLs, DELLA* and *KSN*, with contributions by the effects of phytohormone and starch metabolism.**

Abstract Seasonal plants utilize changing environmental and developmental cues to control the transition from vegetative growth to flowering at the correct time of year. This study investigated global gene expression profiles at different developmental stages of *Rosa odorata* var. *gigantea* by RNA-sequencing, combined with phenotypic characterization and physiological changes. Gene ontology enrichment analysis of the differentially expressed genes (DEGs) between four different developmental stages (vegetative meristem, pre-floral meristem, floral meristem and secondary axillary buds) indicated that DNA methylation and the light reaction played a large role in inducing the rose floral transition. The expression of *SUF* and *FLC*, which are known to play a role in delaying flowering until vernalization, was down-regulated from the vegetative to the pre-floral meristem stage. In contrast, the expression of *VRN1*, which promotes flowering by repressing *FLC* expression, increased. The expression of DELLA proteins, which function as central nodes in hormone signaling pathways, and probably involve interactions between GA, auxin, and ABA to promote the floral transition, was well correlated with the expression of floral integrators, such as *AGL24, COL4*. We also identified DEGs associated with starch metabolism correlated with *SOC1, AGL15, SPL3, AGL24*, respectively. Taken together, our results suggest that vernalization and photoperiod are prominent cues to induce the rose floral transition, and that DELLA proteins also act as key regulators. The results summarized in the study on the floral transition of the seasonal rose lay a foundation for further functional demonstration, and have profound economic and ornamental values.

Keywords Floral transition · Hormones · Sugar metabolism · Photoperiod · *Rosa odorata* var. *gigantea* · Vernalization

Abbreviations

VM	Vegetative meristem
TM	Pre-floral meristem
FM	Floral meristem
VM-DHY	Secondary vegetative meristem
SAM	Shoot apical meristem
DEGs	Differentially expressed genes
GA	Gibberellin
ABA	Abscisic acid
SCL13	Scarecrow-like 13
YUC1	Flavin-containing monooxygenase 1
AUX/IAA	Auxin-induced protein
NCED	9-cis-epoxycarotenoid dioxygenase
KING1/SnRK	SNF1-related protein kinase regulatory subunit gamma-1-like
FKF1	Flavin-binding, kelch repeat, f-box 1
CO	Constans

Electronic supplementary material The online version of this article (https://doi.org/10.1007/s11103-018-0727-8) contains supplementary material, which is available to authorized users.

✉ Qixiang Zhang
zqxbjfu@126.com

[1] Beijing Key Laboratory of Ornamental Plants Germplasm Innovation & Molecular Breeding, National Engineering Research Center for Floriculture, Beijing Laboratory of Urban and Rural Ecological Environment, Key Laboratory of Genetics and Breeding in Forest Trees and Ornamental Plants of Ministry of Education, School of Landscape Architecture, Beijing Forestry University, 100083 Beijing, China

[2] Beijing Advanced Innovation Center for Tree Breeding by Molecular Design, Beijing Forestry University, 100083 Beijing, China

COL	Constans-like
SUS	Sucrose synthase
SS	Starch synthase
GBSS1	Granule-bound starch synthase 1
AMY	Alpha-amylase
BAM	Beta-amylase
AP1	Apetala11
LFY	Leafy
VRN1	Vernalization 1
PEP1	Perpetual flowering 1
AGL	Agamous-like
SOC1	Suppressor of overexpression of co 1
SPL	Squamosa promoter binding protein-like
FLC	Flowering locus c
CAL	Cauliflower

Introduction

Flowering is a pivotal event in the lifespan of ornamental plants, and its timing is precisely mediated by endogenous and exogenous factors that are integrated with finely-tuned regulatory gene networks. Much progress has been made in elucidating the mechanisms underlying floral transition in the model plant, *Arabidopsis thaliana* (Bouché et al. 2016; Kinmonth-Schultz et al. 2016). Indeed, unless stated otherwise, references in this paper to gene names that are not from *Rosa odorata* var. *gigantea* refer to those from *A. thaliana*. To summarize, studies have shown that environmental cues, such as photoperiod or vernalization, and internal factors, including the autonomous pathway, hormonal signaling, age, and sugar metabolism, regulate the expression of a number of floral integrator genes. These genes include *FLOWERING LOCUS T* (*FT*), *CONSTANS* (*CO*), *SUPPRESSOR OF OVEREXPRESSION OF CO1* (*SOC1*), *FLOWERING LOCUS C* (*FLC*), as well as floral meristem identity genes, including *LEAFY* (*LFY*), *APETALA1* (*AP1*), *CAULIFLOWER* (*CAL*), *AGMOUS* (*AG*), and *AGMOUS-LIKE* (*AGL*). The activity of these genes leads to the transition from vegetative to reproductive meristem. Although difference exists in the adaption of different plant species to seasonal cues, the characterization of regulatory networks in experimental model species has laid a foundation to elucidate molecular mechanisms underlying floral transition in both annual and perennial plants (Blumel et al. 2015). Indeed, several studies have provided insights into the molecular mechanisms regulating flowering in perennials species (Fan et al. 2015). Unlike the conversion from vegetative to reproductive meristems in annual plants, this conversion in perennial plants only occurs under favorable conditions, and only certain competent meristems undergo floral transition, while others remain vegetative. Consequently, perennial plants can revert to vegetative growth after flowering.

In temperate regions, most perennial plants flower seasonally, including *Malus*×*domestica*, which blooms in the spring (Kotoda et al. 2006), *Camellia azalea* in the summer (Fan et al. 2015) and *Chrysanthemum lavandulifolium* in the autumn (Fu et al. 2014), while several rose and strawberry species flower continuously under favorable conditions (Iwata et al. 2012). *Malus*×*domestica* completes floral transition prior to winter dormancy (Foster et al. 2003). Unlike other species from the *Camellia* genus, floral transition in *C. azalea* occurs in the spring. Fan et al. (2015) demonstrated that cold, light, and hormone signals converge to regulate floral transition of *C. azalea*. It has been reported that *CO* mRNA accumulation is regulated by circadian rhythm and peaks at the end of the day, while the promoter of *FT* contains CO binding site, and *FT* activity is induced by CO, displaying the circadian rhythm expression pattern. (Böhlenius et al. 2006). *CO* and *FT* are necessary for circadian clock regulation in *A. thaliana* (Blumel et al. 2015). In *Populus trichocarpa* and *C. lavandulifolium*, the "*CO*/*FT* regulatory module" serves similarly as regulators to control the floral transition (Böhlenius et al. 2006; Fu et al. 2014). It was also reported that the specific splicing of the 5′ UTR of the *CiFLC* homolog was closely related to the transformation from juvenile to mature trees (Nishikawa et al. 2007).

Unlike the above examples, some perennials are able to cycle back and forth between vegetative and reproductive growth within a single year. Wang et al. (2009) demonstrated that the expression of *PERPETUAL FLOWERING 1* (*PEP1*), an ortholog of *A. thaliana FLC* gene, was only transiently inhibited by vernalization, and it was activated again when temperatures increased. Whereas the chromatin modification of *FLC* is stable in *A. thaliana*, and this is the reason that annual and perennial plants have different growth behavior. In addition, *PEP1* represses floral transition before vernalization, and facilitates a competence to return to vegetative growth, as well as inhibiting some meristems from completing floral transition, even under inductive conditions. Strikingly, *pep1* mutant plants can flower continuously without the restriction of vernalization, suggesting that *PEP1* regulates its floral transition. In woodland strawberry (*Fragaria vesca*), a 2-bp deletion in the first coding region of *TFL1*, a homolog of *A. thaliana TFL1*, led to recurrent flowering (Iwata et al. 2012). Similarly, Iwata et al. (2012) demonstrated that the transcription of the homolog of *TFL1* in continuous flowering (CF) rose, *KSN*, was disrupted by a *copia*-like retrotransposon insertion, resulting in continuous flowering. Furthermore, Randoux et al. (2014) reported that rose *KSN* acted antagonistically with *FT*, by combining with its partner, *FD*, to repress or promote flowering. *RoTFL1c* is another rose *TFL1* homolog, whose low expression mediates the expression of *LFY*, which in turn

contributes to continuous flowering (Wang et al. 2015). In another study, gibberellin (GA) inhibited the floral transition in the spring of the once-flowering (OF) rose, but did not prevent CF roses from flowering, and cues other than GA are also known to influence rose floral transition (Randoux et al. 2012). Strikingly, the flowering behavior of *Rosa rugosa* 'Hamanasu', a CF rose, was shown not to be controlled by the KSN^{copia} allele (Horibe et al. 2013), indicating that there are other factors that have yet to be identified that regulate this trait. Finally, it has been suggested that CF trait is not a strictly qualitative trait, but rather is qualitative-quantitative (Wang et al. 2015).

Rosa odorata var. *gigantea*, a diploid, evergreen or semi-evergreen perennial liana, and an ancestor of modern roses, has contributed the tea scent and early flowering traits to modern cultivars. At present, little is known about the genetic and molecular basis of floral transition in rose, or how *R. odorata* var. *gigantea* differs from CF roses, for example *R. chinensis* 'Old Blush', in its response to environmental cues. Gene expression patterns involved in the rose floral transition have the potential to elucidate the molecular mechanisms underlying the repeated floral transition in CF roses. In this study, we used a high-throughput sequencing platform to characterize gene expression profiles during floral transition process (vegetative meristem, pre-floral meristem, and floral meristem) and in the secondary axillary buds of *R. odorata* var. *gigantea*. These data sets were combined with observations of concurrent phenotypic and physiological changes (hormone, sugar and starch contents) to provide new insights into the molecular mechanisms underlying the rose floral transition.

Materials and methods

Plant material and experimental procedures

Samples of *R. odorata* var. *gigantea* were obtained from Kunming Yang Chinese Rose Gardening Co., Ltd in the Yunnan Province of China (24°45′N, 102°53′E). In this study, vegetative meristem, pre-floral meristem, floral meristem, and secondary vegetative meristem were abbreviated to VM, TM, FM, and VM-DHY, respectively. The samples of VM, TM, FM stages were collected on December 27, 2014 and January 2 and 9, 2015, respectively, while the secondary axillary buds were obtained on March 8, 2015. It was worth mentioning that the length and width of samples at VM-DHY point was almost similar to the samples at TM point. Three biological replicates were collected for each stage, with each sample being obtained from one individual plant. Scales and young leaves outside of the buds were peeled off as much as possible, so that the remaining tissue was closer to shoot apical meristem, and each sample contained approximately 25–30 pooled buds (~0.3 g). All samples were collected during the time from 12:00 to 17:00, immediately transferred to liquid nitrogen, and stored at −80 °C until further use. Samples for paraffin sections, RNA extraction, hormone, soluble sugar, and starch measurements were concurrently collected. The lengths and widths of 20 randomly selected axially buds were measured.

Microscope observations

Axillary buds peeled off bracts and young leaves were cut off, then immediately fixed in an FAA solution (formalin: acetic acid: 50% ethanol = 5/5/90 v/v). Fixed samples were first dehydrated with a graded ethanol series (50–100%) and xylene, and then embedded in paraffin (Sigma), and the paraffin was removed from 8 μm thick sections (Lecia Microtome, Wetzlar, Germany) with xylene. The sections were then hydrated in a series of solutions with decreasing ethanol concentration (100–50%), and stained with Safranin and Fast Green (Sigma). Sections were sealed using neutral gum and visualized using a Scope A1 microscope (Zeiss, Jena, Germany).

Measurements of soluble sugar, starch, and hormone contents

Fresh samples of approximately 0.1 g at four developmental stages were collected for the measurement of soluble sugars and starch, and with at least 50 mg for the hormone measurements. The internal standards used in this study are listed in Table S1. The soluble sugar and starch contents were measured using the sulfuric acid-anthrone colorimetric method (He 1985). High-performance liquid chromatography-mass spectrometry (HPLC - MS) (AB 5500, Beijing, China) was used to identify and quantify hormones as previously described (Pan et al. 2010).

RNA extraction, sequencing and library construction

Total RNA was isolated with an EasySpin RNA Reagent (Aidlab, Beijing, China) according to the manufacturer's instructions, then reverse transcribed into cDNA using random primers. Second strand cDNA was subsequently synthesized using buffer, dNTPs, RNase H, and DNA polymerase I. The library fragments were purified with AMPure XP system (Beckman Coulter, Beverly, USA), end repaired, poly (A) tailed, and ligated to Illumina sequencing adapters. After quantification and qualification, the ligation products were sequenced using an Illumina HiSeqTM 4000 platform.

De novo assembly and annotation

After filtering raw reads, clean reads were de novo assembled using the Trinity short reads assembling program (Grabherr et al. 2011), resulting in a transcriptome reference database. All sequence data were deposited in the Genome Sequence Archive with the project ID PRJCA000286. The unigene expression values were calculated and normalized to RPKM (Reads Per kb per Million reads) (Mortazavi et al. 2008). A differential expression analysis between stages was performed using the ratio of RPKM values, and the p-value correction (false discovery rate, FDR) was adjusted using the Benjamini and Hochberg method (Thissen and Kuang 2010). The differentially expressed genes (DEGs) between any two stages were determined using $\log_2 > 1.0$ and FDR < 0.05. Unigenes were annotated using BLASTx with an E-value threshold of $1e^{-5}$ to Nr, Swiss-Prot protein, Kyoto Encyclopedia of Genes and Genomes (KEGG), and KOG database, respectively, and protein functional annotations were assigned based on the best alignment results (Moriya et al. 2007; Young et al. 2010). The protein coding sequences of the unigenes were aligned using a BLASTx search in the Plant TFdb v 3.0 (http://planttfdb.cbi.pku.edu.cn) database (Jin et al. 2015), and transcription factors (TFs) that were expressed between VM and TM were identified.

The web-based ReviGO software (http://revigo.irb.hr) was used to reveal enriched gene ontology (GO) functional categories identified from each comparison (Supek et al. 2011). DEGs were annotated using the Mercator web tool (Lohse et al. 2014) and then analyzed using the MapMan software (Usadel et al. 2009) to reveal putative functional enrichment.

Data validation by real-time quantitative PCR (RT-qPCR)

RT-qPCR was performed using a qTOWER 2.2 PCR System (Jena, Germany) and SYBR Green PCR Master Mix (Takara, Dalian, China) according to the manufacturer's protocol. Total RNA treated with DNase (Takara, Dalian, China) was reverse transcribed to produce cDNA templates for reactions according to the manufacturer's instructions (Takara, Dalian, China). The primer sequences for RT-qPCR were designed using the PrimerQuest Tool (Table S2), and synthesized by Sangon Biotech Co., Ltd. (Beijing, China). The *RcActin* gene was used as a reference gene (Dubois et al. 2011). Each 20 µL reaction mixture contained 2 µL cDNA template. The amplification program was as follows: 3 min at 95 °C and 40 cycles of 10 s at 95 °C and 30 s at 60 °C. Relative expression levels of candidate genes were calculated using the $2^{-\Delta\Delta C_t}$ method (Schmittgen and Livak 2008). Each reaction was performed with three biological replicates. Pearson's correlation values between RNA-seq and RT-qPCR data of 14 selected genes were calculated using cor. test in R version 3. 3. RNA-seq data were Log-transformed prior to the Pearson's correlation determination.

Co-expression analysis of TFs and floral candidate genes

The Pearson's correlation coefficient values between pairs of genes were calculated with the 'Hmisc' package. Correlations corresponding to a coefficient with $|r| > 0.8$ and p-value < 0.05 were selected (Table S3). The co-expression network of TFs and key candidate floral genes was visualized using Cytoscape version 3. 3. 0.

The packages of 'VennDiagram' and 'pheatmap' and Hclust function were used to produce venn diagrams, heatmaps and hierarchical clustering analysis respectively in R version 3. 3. Data were normalized by their Z-scores before pheatmap and Pearson's correlation analyses.

Results

Morphological identification and physiological measurement of the different rose developmental stages

In terms of the morphological changes in the SAM, the floral transition process was divided into vegetative meristem (VM), pre-floral meristem (TM), and floral meristem (FM) (Fig. 1a). No obvious differences in the external phenotypes of the buds were observed during the rose floral transition process (Fig. S1A). When measuring the length and width of the axillary buds, the ratio of length divided by width gradually decreased (Fig. S1A). At VM stage, the ratio of length to width was 1.20, the shape of meristems was narrow (Fig. 1a). At TM stage, the SAM became broader and hunched into a conical dome, displaying the evidence of a transition to a floral meristem (Fig. 1a). This stage was therefore named the floral transition stage (pre-floral meristem), as the buds were preparing to transform from vegetative to reproductive growth. At FM stage, the ratio of length to width was 0.88 and sepal primordia on the flank of SAM developed into sepals (Fig. 1a). Subsequently, the buds sequentially developed petals, stamens, and pistils (Fig. S1B). After flowering, secondary axillary buds sprouted, but did not develop flowers again (Fig. S1A). The morphological characters of the secondary axillary bud apex were typical of a vegetative meristem (Fig. 1a), similar to a VM.

The content of hormones, soluble sugar and starch were measured during the floral transition process (VM, TM, and FM) and in the secondary axillary buds (VM-DHY). As shown in Fig. 1b, the levels of GA_1, GA_3, and GA_4,

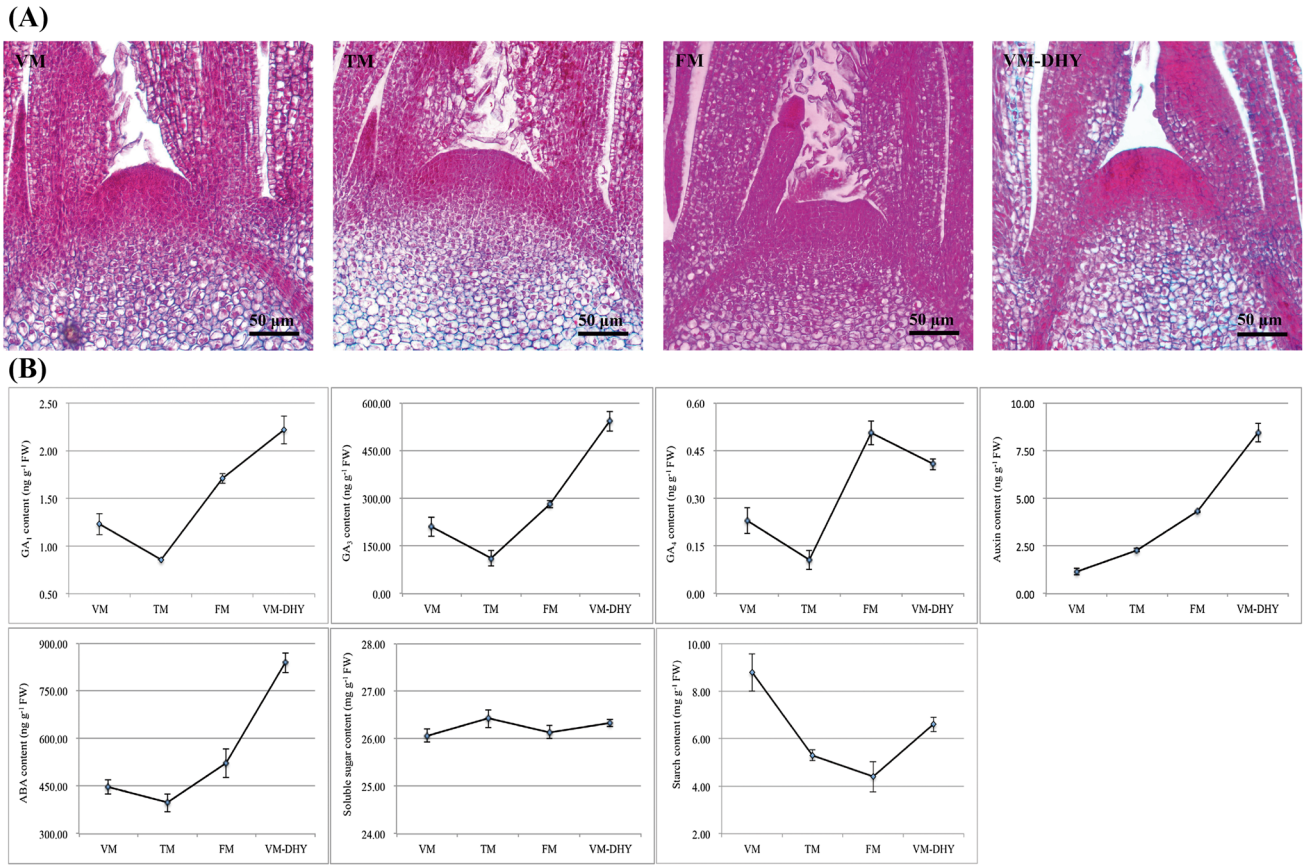

Fig. 1 Morphological and physiological characteristics of SAM during different developmental stages in *Rosa odorata* var. *gigantea*. **a** Morphological changes were analyzed at a histological level: *VM* vegetative meristem, *TM* pre-floral meristem, *FM* floral meristem, *VM-DHY* vegetative meristem in axillary buds. **b** The contents of hormones, soluble sugar and starch in different developmental stages of *R. odorata* var. *gigantea*. GA_1, GA_3, GA_4, IAA, ABA, soluble sugar, starch. Values are means of three replicates ± SE

decreased from VM to TM, but had the highest in VM-DHY sample. In contrast, the levels of auxin increased from VM to TM, and reached a maximum at VM-DHY stage (Fig. 1b). Abscisic acid (ABA) levels decreased from VM to TM, and were high between FM and VM-DHY. We observed almost no change in soluble sugar contents during the four developmental stages (Fig. 1b), while the SAMs of non-induced plants had higher starch contents than those of induced SAMs (Fig. 1b). Compared to VM, the content of starch

Table 1 Throughput and quality of RNA-seq

Library	Raw reads	Clean reads	Q20 (%)	Q30 (%)	GC content (%)
VM_DH1	58626276	56681860	96.71	92.88	46.26
VM_DH2	59886500	58039272	96.73	92.87	92.87
VM_DH3	85411974	79152152	97.56	94.03	47.58
TM_DH1	85600288	79010260	97.43	93.80	48.38
TM_DH2	92265032	84146886	97.35	93.63	46.08
TM_DH3	90206512	82748564	97.31	93.52	47.80
FM_DH1	85861790	79768252	97.52	93.95	47.86
FM_DH2	57721822	55158226	95.30	89.95	47.79
FM_DH3	88496002	80681866	97.22	93.30	47.27
VM_DHY1	98245216	90663928	97.48	93.87	47.57
VM_DHY2	58118508	56410814	96.14	91.48	47.86
VM_DHY3	55082328	54039034	95.05	89.76	47.48

decreased by ~39.8% at TM, and by ~50.0% at FM, but increased in the VM-DHY (Fig. 1b).

Sequencing, de novo assembly and annotation of the rose transcriptome

Twelve cDNA libraries corresponding to four developmental stages (VM, TM, FM, and VM-DHY) were constructed for RNA sequencing. A total of 915,522,248 raw reads were generated, after low-quality reads and adapter sequences had been removed, a total of 856,501,114 clean reads were used for further analysis (Table 1). De novo assembly of the reads yielded a total of 97,115 unigenes with a mean size of 864 bp (Fig. S2A). Of the unigenes, 52.7% were annotated by at least one database with an E-value threshold $< 10^{-5}$. 11,992 unigenes were annotated collectively using the Nr, Swiss-Prot, KOG and KEGG public databases (Fig. S2B). As shown in Fig. S3A, 32,331 unigenes were annotated to 4 top-hit species, including *Fragaria vesca* subsp. *vesca, Prunus mume, Malus domestica* and *Pyrus*×*bretschneideri*. Unigenes that were not similar to any genes in the public database were further predicted ORF information using ESTscan (3.0.3) software. The results showed that a total of 3,525 unigenes owned predicted ORF, of which 1, 711 unigenes had ORF longer than 100 amino acids (Fig. S3B). A distribution of functional classifications of the annotated unigenes was made using the gene ontology (GO) and KEGG databases (Fig. S4).

To evaluate the reproducibility between biological replicates and the correlation between samples, correlation

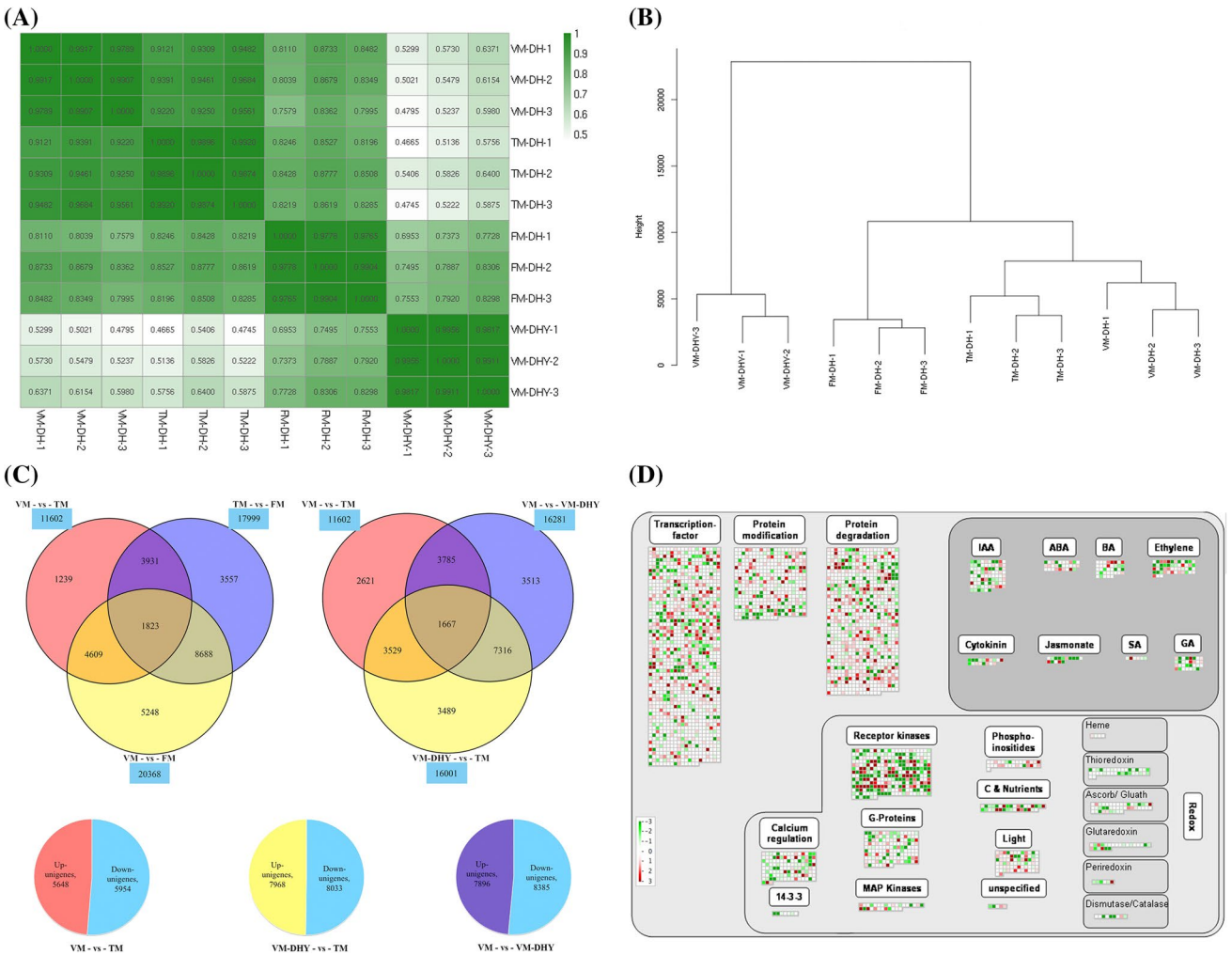

Fig. 2 Relationship of transcriptomic samples, number of DEGs in each comparison, and MapMan metabolism overview maps between VM and TM. **a** Distribution of correlation co-efficiencies between each pair of samples. **b** Hierarchical clustering showing global relationships of samples between different developmental stages based on Euclidian distance. The y-axis shows the degree of the variance. **c** Number of DEGs with conserved and meristem-phase specific expression in the four developmental stages. **d** MapMan metabolism overview maps showing differences in transcript levels between VM and TM. The color indicated $\log_2$ value of fold changes, blue represents down-regulated transcripts, and red represents up-regulated transcripts

analysis, hierarchical clustering analysis and principal component analysis (PCA) of the expression data were performed (Fig. 2a, b and Fig. S5). We observed a close correlation between biological replicates of each stage. Additionally, the data from VM and TM samples clustered in close proximity, while VM-DHY samples were clearly distinguishable from other stages, suggesting the division of stages was accurate.

Identification of DEGs through development

DEGs were identified by pairwise comparison of different stages (Fig. 2c). From these comparisons, 11,602, 17,999, 20,368, 16,281 and 16,001 DEGs could be distinguished from VM versus TM, TM versus FM, VM versus FM, VM versus VM-DHY, and VM-DHY versus TM comparisons, respectively. We identified 5648 unigenes with a higher expression and 5954 with a lower expression in VM versus TM (Fig. 2c). Likewise, 7968 and 7896 unigenes showed higher expression, and 8033 and 8385 showed lower expression in VM-DHY versus TM and VM versus VM-DHY, respectively (Fig. 2c). The number of DEGs identified in VM-DHY versus TM was higher than in VM versus TM (Fig. 2c). Strikingly, 16,281 genes were differentially expressed between VM and VM-DHY. Considering environmental cues, we speculated that DEGs involved in vernalization and photoperiod might be related with the difference between VM and VM-DHY. Functional categorization of the DEGs from VM versus VM-DHY were analyzed using the MapMan software, revealing a high proportion of genes from the TF, protein modification, and protein degradation categories. Furthermore, genes associated with auxin, ABA, GA, light regulation, as well as receptor kinases, were enriched, indicating that photoperiod or temperature may affect hormone metabolism and further regulate the rose floral transition (Fig. 2d).

GO analysis of DEGs related specifically to floral transition

DEGs identified from VM versus TM, TM versus FM, VM versus VM-DHY, and VM-DHY versus TM comparisons, were annotated by GO analysis to examine putative functional differences between different developmental stages. Based on previous studies of flowering transition (Blumel et al. 2015; Khan et al. 2014), we focused on genes involved in photoperiod, hormone signals, vernalization, autonomous and sugar metabolism pathways. The relevant GO terms (FDR < 0.25) for each comparison were identified (Table S4) and were further visualized using the ReviGO tool (Supek et al. 2011) (Fig. 3). The enriched GO terms from VM versus TM and VM-DHY versus TM comparisons were similar and related to photosynthesis, light reaction, sugar metabolism and hormones metabolic process (Fig. 3a, c). Interestingly, the DNA methylation and histone lysine methylation terms were significantly enriched in DEGs identified from VM versus TM and VM-DHY versus TM comparisons, respectively. Photosynthesis, light reaction, and carbon fixation terms were intensely enriched in VM versus VM-DHY (Fig. 3d). The demethylation, histone demethylation and reproduction terms were only enriched in TM versus FM (Fig. 3b). These differences were mainly consistent with gene expression profiles from each comparison, indicating that exogenous and endogenous cues are integrated to mediate the rose floral transition, and that DNA methylation has a significant influence on flowering.

DEGs associated with hormones

We identified DEGs involved in hormone biosynthesis and metabolism and signal pathways. The DEGs, *KAO1* and *GA20ox*, which are predicted to participate in active GA biosynthesis, showed higher expression at VM than at TM, and were highly expressed at VM-DHY. In contrast, the *GA2ox7* and *GA2ox8* genes, which are associated with GA-deactivation, showed higher expression both at VM and TM than at VM-DHY (Fig. 4a). The expression of these genes contributes to low levels of GA. The expression of *GID1B* and *GID1C*, involved in GA-mediated signaling pathway, decreased from VM to TM, whereas *GID2*, encoding a putative F-box protein that is a component of Skp 1p-cullin-F-box protein (SCF) complex, showed high expression during flower transition. DELLA proteins are known to be central nodes in the GA signaling pathways, and we observed that the expression of the DELLA protein RGL1 increased from VM to TM. The homolog of *Gibberellic Acid-stimulated in Arabidopsis* (*GASA*) also had high expression levels during floral transition (Fig. 4a). These changes in expression likely converged into a GA response that regulated floral transition, and the activity of the GA response further modulated GA biosynthesis via a feedback loop, affecting the concentration of active GA (Hedden and Thomas 2012). Taken together with the change of GA contents, we concluded that GA suppresses the rose floral transition.

The expression of auxin biosynthetic genes including indole-3-pyruvate monooxygenase (*YUCCA2*), FMO-flavin monooxygenase (*YUC10*), IAA-amino acid hydrolase (*ILR1*), and auxin signaling F-Box protein (*AFB2*) was up-regulated in VM versus TM than in VM versus VM-DHY (Fig. 4b). Indole-3-acetic acid-amido synthetase (*GH3*) regulates the conjugation of auxin to amino acids, maintaining auxin homoeostasis (Kang et al. 2013). Here, *GH3.1* and *GH3.6* expression increased from VM to TM, indicating auxin synthesis. Multiple members of the AUX/IAA protein families, including *IAA4, IAA14, AUX15A, AUX1*,

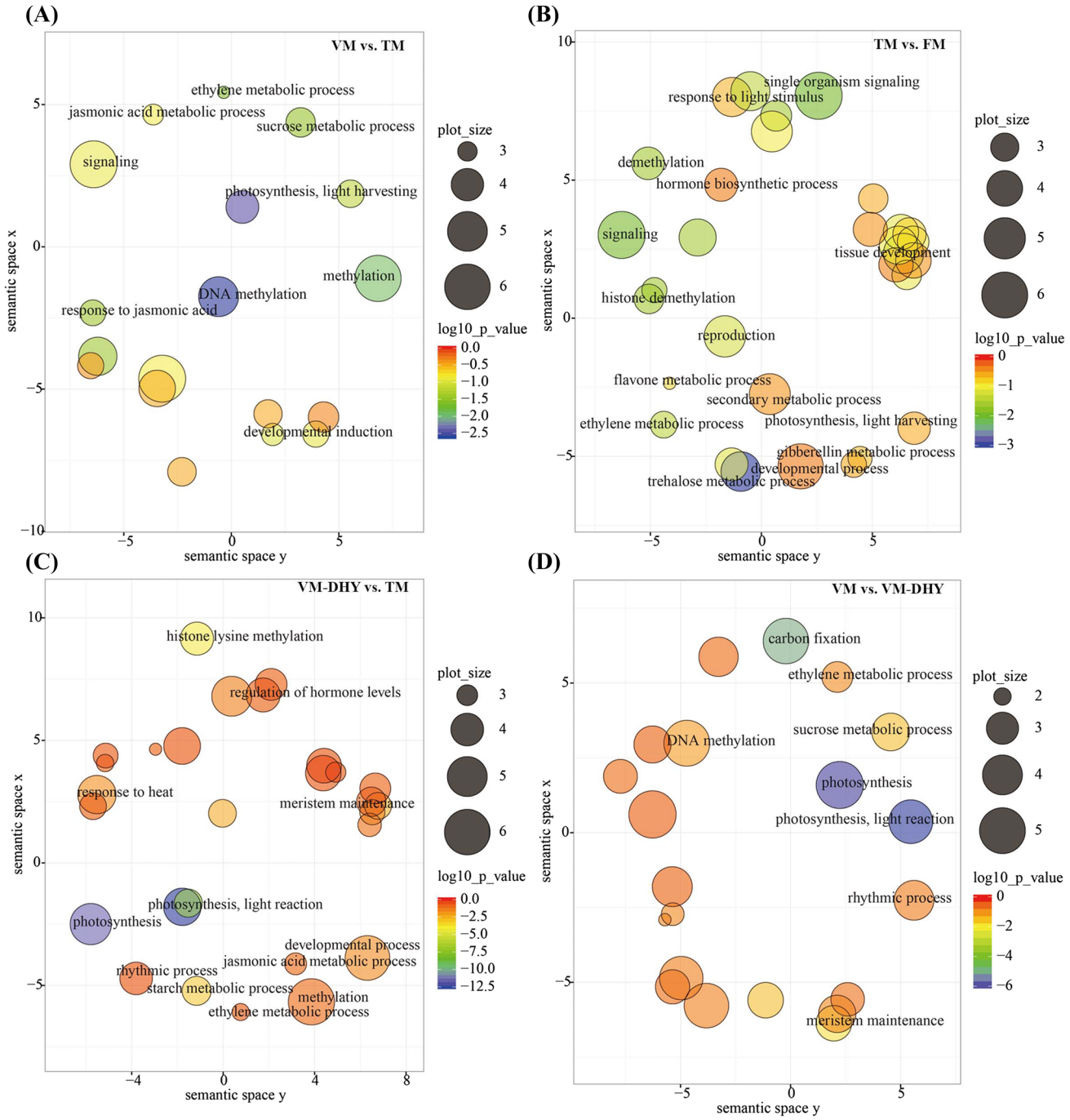

Fig. 3 Scatterplot of enriched GO terms largely associated with flower transition between developmental stages. **a** The scatterplot of enriched GO terms between VM and TM stage; **b** The scatterplot of enriched GO terms between TM and FM stage; **c** The scatterplot of enriched GO terms between VM-DHY and TM stage; **d** The scatterplot of enriched GO terms between VM and VM-DHY stage. Bubble color indicates the p-value of GO term; bubble size indicates the frequency of the GO term in the underlying GOA database

and *AUX28*, showed low expression during floral transition, but were highly expressed at VM-DHY. In contrast, auxin response factor 18 (*AFR18*), had a high expression during floral transition. Each AUX/IAA protein is known to repress a specific ARF partner (Kang et al. 2013), and hierarchical clustering analysis (Fig. 4b) indicated potential functional pairs based on co-expression between *AUX/IAA* and *ARF*, specifically *AUX15A* and *ARF18*, and *IAA14* and *ARF8*. Additionally, *AUX/IAA* showed reduced expression during floral transition and had the highest expression at VM-DHY stage. Plant-specific pin-formed (PIN) protein had similar expression patterns to IAA/AUX proteins at different

developmental stages, suggesting that the contents of auxin increased during the rose floral transition, consistent with the measurement outcome of auxin content at different developmental stages (Fig. 1b). So auxin may promote the rose floral transition.

The ABA biosynthetic gene, 9-cis-epoxycarotenoid dioxygenase (*NCED3*) decreased from VM to TM, but had high expression at VM-DHY, while the metabolic gene, abscisic acid 8′-hydroxylase (*ABAH*), was just opposite (Fig. 4c). ABA receptors, *PYR1, PYL4, PYL9*, and *PYL12*, had low expression levels during the rose floral transition, and which are known to combine with protein phosphate 2C (*PP2C*) and directly mediate PP2C phosphatases, which in turn directly regulate SNF1-related protein kinases (*SnRK*) (Cutler et al. 2010). Here the expression of *SnRK* decreased from VM to TM, implying that ABA plays a role in suppressing floral transition. Based on gene co-expression and hierarchical clustering, *ABAH2* and *PP2C16, PYL12* and *SnRK* were shown to have similar expression patterns, suggesting that genes associated with the metabolism, perception, and activity of ABA were involved in floral transition (Fig. 4c).

DEGs associated with sugar and starch metabolism

DEGs representing sugar transportation and metabolism were identified in all comparisons, collectively indicating that trehalose-6-phosphate (T6P) and starch metabolism played an important role in inducing the rose floral transition. Sucrose movement is known to be mediated by sugar transport proteins, such as SUC2, SUC3, SUT5, SUT13, and ERD6, which were all up-regulated from VM to TM. Intracellular sucrose is further cleaved by alkaline/neutral invertase (A/N InV), creating glucose and fructose, or transformed by sucrose synthase (*SUS*), generating UDP-glucose (*UDPG*) (Fig. 4d). Glucose can then be converted to T6P by trehalose-6-phosphate synthase 1 (*TPS1*), which was up-regulated from VM to TM, but showed lower expression at VM-DHY (Fig. 4d). T6P can also be hydrolyzed by trehalose-phosphate phosphatase (*TPP*), releasing trehalose (Lastdrager and Smeekens 2014). *TPP* showed a lower expression during floral transition process than TM and VM-DHY stage respectively.

Starch synthase 4 (*SS4*) and granule-bound starch synthase1 (*GBSS1*) both had higher expression at TM than at VM, and the lowest expression levels at the VM-DHY stage (Fig. 4d). DEGs associated with starch breakdown were also identified, including alpha-amylase (*AMY*), beta-amylase (*BAM*), and isoamylase (*ISA*), and all showed greater expression during floral transition than at VM-DHY stage.

DEGs involved in flowering pathways

Photoperiod induces floral transition by means of circadian clock to response to the duration of day or night. As shown in Fig. 4e, the far-red elongated hypocotyl 3 (*FHY3*) and far-red impaired response (*FRS1-3, FRS5, FRS9*) genes showed higher expression levels during floral transition process than at VM-DHY stage (Fig. 4e). These genes are known to promote a photoreceptor, phytochrome A (*phyA*), which is triggered by both red light and far-red light (Hararisteinberg et al. 2001). *PhyA*, promoting the expression of *CO* (Fornara et al. 2010), increased from VM to TM, whereas the E3 ubiquitin-ligase *CONSTITUTIVE PHOTOMORPHOGENIC 1* (*COP1*) inhabits flowering by promoting the degradation of CO through the proteasome in the dark at the post-transcriptional level (Fornara et al. 2010). Here, *COP1* decreased from VM to TM, while the expression of *COL1, COL4, COL5, COL13, COL15*, which are homologs of *CO*, were just the opposite (Fig. 4e). *EARLY FLOWERING 3* (*ELF3*) is also more highly expressed in the afternoon, and induces the expression of *LATE ELONGATED HYPOCOTYL* (*LHY*) and early light-induced protein 1 (*ELIP1*) (Yu et al. 2009). We observed that *LHY* and *ELIP1* increased during floral induction process, and had higher expression than at VM-DHY. Taken together, photoperiod (circadian clock) probably functions as an activator to promote the transition from vegetative to reproductive growth.

In addition to photoperiod, vernalization is another major stimulus for triggering seasonal plants to flower. Prolonged winter cold was previously shown to lead to inhibition or epigenetic silencing of *FLC*. *FRIGIDA* (*FRI*) interacts with *SUPPRESSOR OF FRI4* (*SUF4*), and promotes the expression of *FLC*. In this study, *FRI5* and *SUF4* expression decreased from VM to TM (Fig. 4e), while *VERNALIZATION 1* (*VRN1*) and *VERNALIZATION INSENSITIVE 3* (*VIN3*), which are known to contribute to the silencing of *FLC*, showed higher expression during floral transition process than at VM-DHY. It is noteworthy that *VRN1*, a homolog of *AP1*/*FUL* in *A. thaliana*, directly induces floral transition (Kim et al. 2009). Additionally, *FY*, an autonomous pathway gene, which also reduce *FLC* expression (Khan et al. 2014), increased from VM to TM. Ultimately, the expression of *FLC* decreased from VM to TM, and likely enabled the completion of floral transition.

In this study, we examined the expression patterns of key genes associated with floral transition from vegetative to reproductive meristem. Meristem maintenance is controlled by a negative feedback loop involving *WUSCHEL* (*WUS*) and *CLAVATA3* (*CLV3*), which is one member of the *CLAVATA3*/*ESR* (*CLE*) family (Zhao et al. 2004). Additionally, the *WUS* signaling pathway is regulated by the

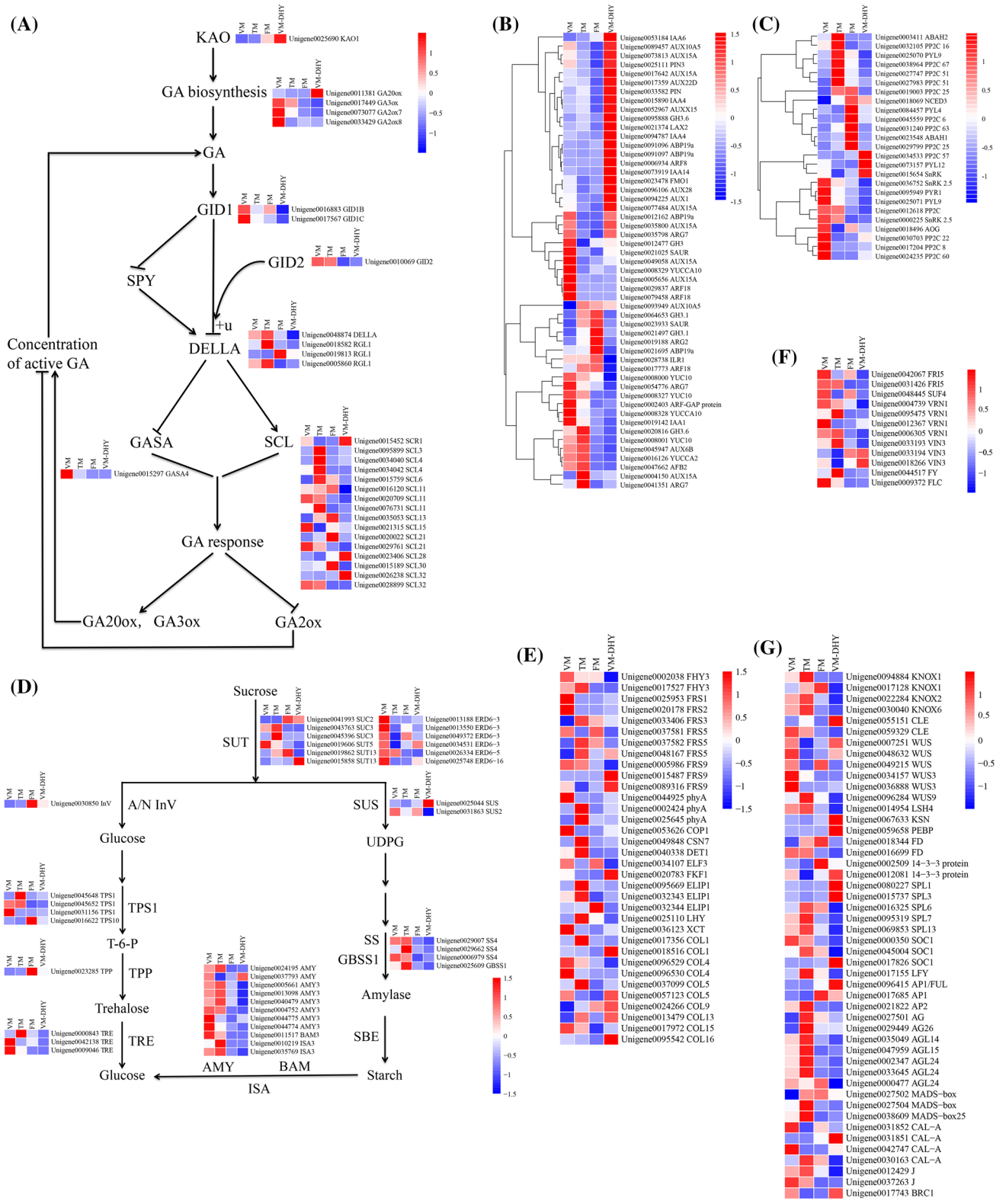

intercellular signal of CLE peptide (Zhao et al. 2004). In the present study, the expression of *CLE* was up-regulated in VM vs. TM, whereas the expression of *WUS* decreased, and showed the highest at VM-DHY (Fig. 4g). Another meristem maintenance gene, *KNOTTED1-LIKE HOMEOBOX* (*KNOX*) was up-regulated in VM versus TM. Importantly, *KSN*, described in the introduction, which belongs to the phosphatidylethanolamine-binding protein (PEBP)

◂**Fig. 4** DEGs involved in different floral pathways in different developmental stages. **a** Expression patterns of DEGs involved in GA metabolism and signal pathway in different developmental stages. **b** Hierarchical clustering analysis of DEGs involved in IAA metabolism and signal pathway in different developmental stages. **c** Hierarchical clustering analysis of DEGs involved in ABA metabolism and signal pathway in different developmental stages. **d** Expression patterns of DEGs involved in sugar metabolism pathway in different developmental stages. **e** Expression patterns of DEGs involved in photoperiod pathway in different developmental stages. **f** Expression patterns of DEGs involved in vernalization pathway in different developmental stages. **g** Expression patterns of DEGs associated with floral integrators in different developmental stages. Data for gene expression level were normalized by Z-score, Red and blue colors represent up- and down- regulated genes, respectively

family, had lower expression during floral transition, but higher at the VM-DHY stage. Expression of microRNAs, *MiR156* and *miR172*, which modulates the expression of *AQUAMOSA PROMOTER BINDING PROTEIN-LIKE* (*SPL*) genes (Khan et al. 2014), *SPL6, SPL7* and *SPL9*, increased from VM to TM, but *SPL1* and *SPL3* had the highest expression level at VM-DHY. The expression of key floral integrators and floral meristem identity genes, such as *SOC1, LFY, AP2, AG, AG26, AGL14/15, AGL24, CAL-A*, as well as other *MADS*-box genes, increased during floral transition, and showed lower expression at VM-DHY stage (Fig. 4g). Taken together these data suggest that they are candidate genes mainly associated with the rose floral transition.

Candidate genes significantly associated with the rose floral transition

With the above background, we selected several key genes belonging to hormone (GA, auxin, and ABA) signals, sugar metabolism, photoperiod, and vernalization pathways, and further compared their expression patterns in pairwise comparisons (VM vs. TM, VM-DHY vs. TM, TM vs. FM, and VM-DHY vs. VM). As shown in Fig. 5a, based on expression profiles in each comparison of DEGs involved in each pathway, we summarized that auxin, sugar metabolism, photoperiod, and vernalization pathways functioned as activators to promote floral integrators, including *SPL6/13, SOC1, LFY, AG, AGL14/15/24, CAL-A*, and *MADS-box 25* and so on. Conversely, GA and ABA pathways inhibited the rose floral transition. Taken together, a hypothetical regulatory network controlling the rose floral transition, involving all these pathways, is proposed in Fig. 5b.

TFs involved in the rose floral transition

Based on a BLASTx search of the Plant TFdb (Jin et al. 2015), a total of 153 genes were identified as transcriptional regulators with differential expression between VM and TM stage (Table S5). These were further divided into different gene families (Fig. 6a), and a total of 26, 22, 11 and 11 unigenes assigned to the *ERF/AP2, WRKY, B3* and *NAC* families, respectively. The *WUS/WOX3* TFs from the *WOX* family were down-regulated from VM to TM (Fig. 4g and Table S5), which mediate meristem maintenance (Zhao et al. 2004). In addition, *WUS* also can combine with *LFY* to promote *AG* expression in flower buds (Lenhard et al. 2001). *SCL* genes belong to GRAS TF family and function as a downstream suppressors of GA signaling (Zhang et al. 2011). *SCL3, SCL13* and *SCL21* increased from VM to TM (Fig. 4a), indicating that they may promote floral transition. In contrast the expression of the four *MYB* family TFs decreased from VM to TM (Table S5), suggesting a role in suppressing floral transition. Functional categorization using MapMan software showed that TF genes were strongly enriched in the DEGs associated with VM vs. TM comparison (Fig. S6A). For example, the floral meristem identity genes, *LFY* and *CAL-A*, belong to *LFY* and M-type families respectively, which are known to promote the transition from vegetative to reproductive growth. Here, *LFY* and *CAL-A* increased from VM to TM (Fig. 4g), consistent with their role in promoting the rose floral transition. *VRN1* and reproductive meristem (*REM5*) were assigned to the B3 family and increased from VM to TM (Table S5). *VRN1* is proposed to participate in the epigenetic expression of *FLC* and promote floral transition (Khan et al. 2014). Other TFs from families such as *ERF/AP2, WRKY* and *NAC* were also differentially expressed between VM and TM (Table S5), indicating that they contribute to floral transition, but further experiments are needed to demonstrate their regulatory function.

Co-expression of TFs with floral integrators

Based on the concept of 'guilt by association' (Wolfe et al. 2005), high co-expression between pairs of genes indicates that these genes have a similar expression 'behavior' in the same biological process. To apply this idea to our dataset, we calculated the Pearson correlation coefficient (r) between TFs (Fig. 6a) and key candidate floral genes, such as *SOC1, LFY, AGL24, COL1, KSN, FLC* and so on, whose expression were significantly associated with floral transition (Table S3). When we observed a p-value < 0.05 and $|r| > 0.8$ between pairs of genes, we speculated that these genes had highly synergistic or antagonistic co-expression behavior, and their proposed interactive action was analyzed using the Cytoscape software. As shown in Fig. 6b, *MYB* and *bHLH14* were putative suppressors with expression levels that showed a highly negative correlation to

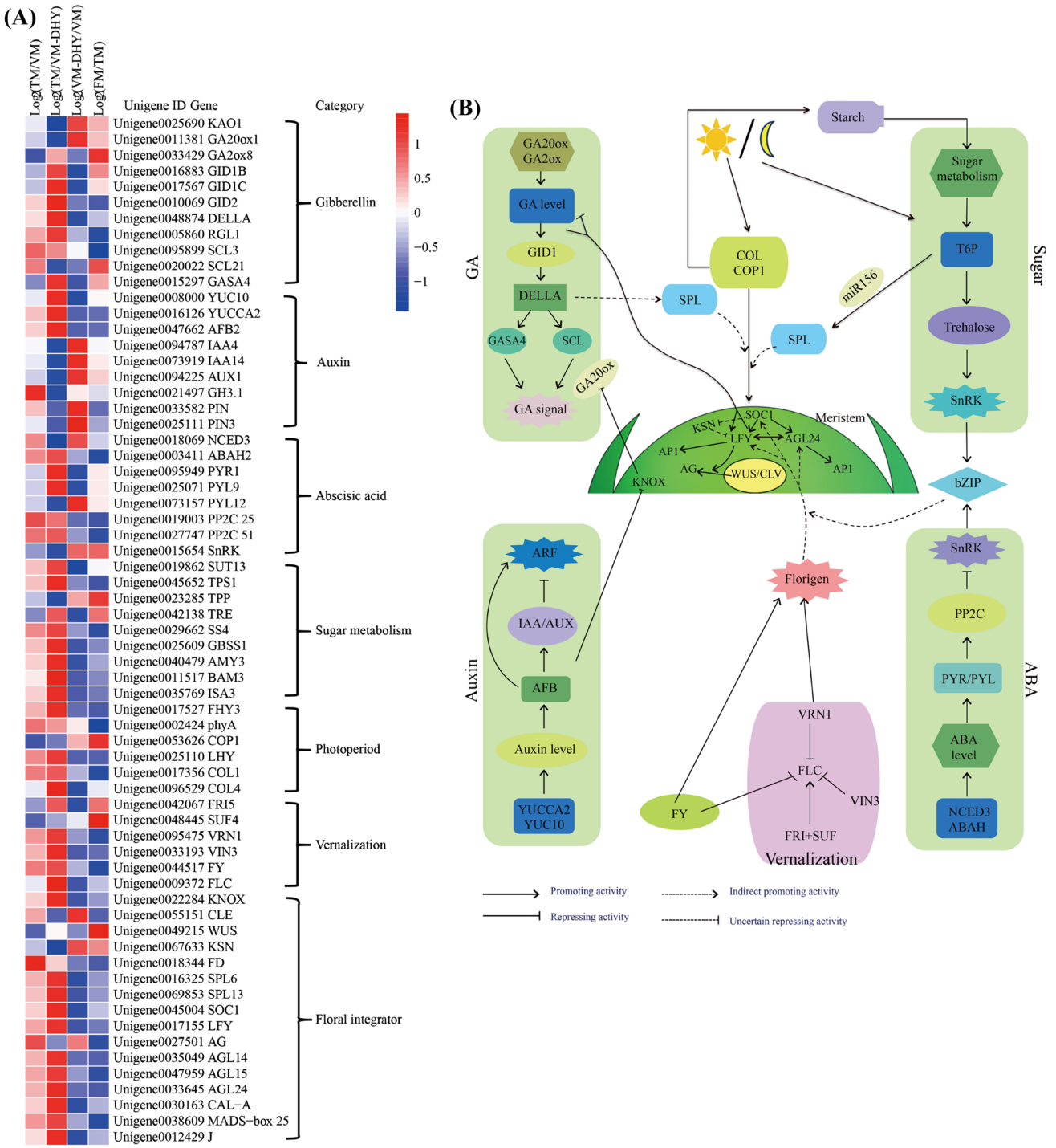

Fig. 5 Key candidate genes associated with floral transition. **a** Heatmap of DEGs mainly associated with floral transition in the rose. Data for gene expression level were normalized to Z-score, Red and blue colors represent up- and down- regulated genes, respectively. **b** A hypothetical model for the regulatory network of the rose floral transition. Arrow indicates a promoting activity, T-end indicates repressing activity. Dashed lines show an indirect interaction

those of key floral candidates, but *bHLF191* showed good expression correlation. TFs, *SCL13* and *SCL21*, belonging to GA signal pathway, showed good correlation with *MYC2* and *bHLH35*, suggesting that *MYC2* and *bHLH35* may be involved in GA signal transduction. Finally, *KSN* showed a negative correlation with sugar metabolic genes, including *GBSS1, ISA3, AMY3* and *SPL3*, while *GBSS1* positively correlated with *SOC1* and *SPL3*, which is

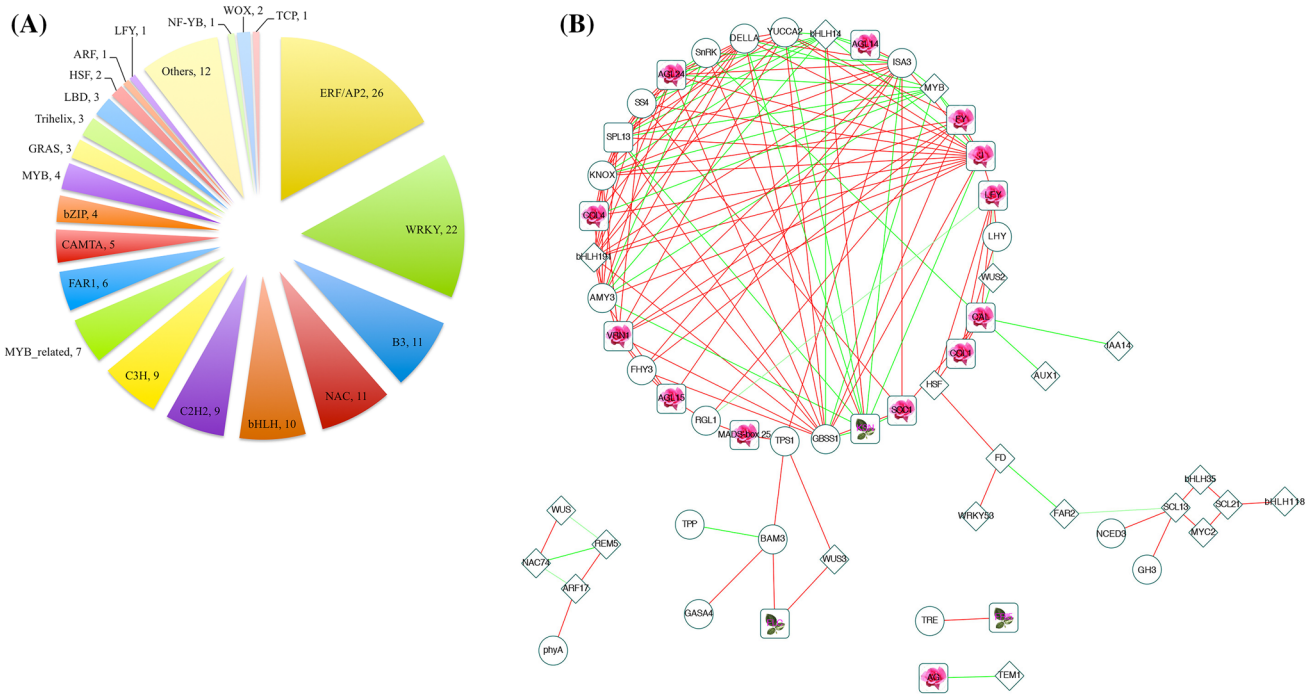

Fig. 6 Classification of TFs and co-expression network of transcription factors (TFs) and candidate floral genes during the rose floral transition. **a** The family assignment of 153 TFs during the rose floral transition. Number of genes assigned to each family was shown behind a comma. **b** Co-expression network of TFs and candidate floral genes during the rose floral transition. Round rectangle nodes represented key floral integrators, Ellipse nodes represented candidate floral genes, and diamond nodes represented transcription factors. Red lines represented positive correlation, and green lines represented negative correlation between pairs of genes. Only pairs of genes with correlation coefficient (|r|) > 0.8 and p-value < 0.05 were shown

congruent with the idea that starch metabolism is involved in controlling floral transition.

Verification of gene expression through RT-qPCR

To confirm the reliability of the RNA-seq data, we selected 14 candidate DEGs, belonging to vernalization, photoperiod and GA pathways, for parallel RT-qPCR based expression analysis. The results obtained by RT-qPCR and RNA-seq were similar, confirming the accuracy of our transcriptomic analysis (Fig. 7).

Discussion

Hormone signaling mediates flowering transition in rose

We observed that the content of GA and the expression of associated biosynthetic genes decreased during the rose floral transition (Figs. 1b, 4). Previous genetic inheritance studies have shown that plant architecture is associated with flowering behavior, and that a few genes involved in the biosynthesis of GA and auxin have been found in the vicinity of quantitative trait loci (QTLs) that are known to control rose phenotypes, including plant form and flowering behavior (Kawamura et al. 2015), suggesting that hormones are involved in regulating rose floral transition. It has been demonstrated that GA acted positively then negatively to control floral transition in *A. thaliana*. Initially, *LFY* was promoted by GA, then increasing *LFY* expression reduced GA levels in a negative feedback loop, permitting the accumulation of DELLA, which in turn activated *AP1* expression to control the onset of the flowering transition (Yamaguchi et al. 2014). In this study, the expression of *DELLA, RGL1, SCR*, and *SCL* genes increased during floral transition (Fig. 4a) and *DELLA* expression correlated well with the expression of *AGL24*, but showed a negative correlation with *KSN* (Fig. 6b), suggesting that *DELLA* promotes floral transition. Similar results were reported in cherry (*Prunus avium*) and *Citrus unshiu* (Boss and Thomas 2002; Nishikawa et al. 2009). Additionally, Yu et al. (2012) reported that *DELLA* interacted with *SPL* through *miR156*, and controlled the expression of *SPL* and *MADS-box* genes in *A. thaliana*. We observed that the expression of *DELLA, RGL1, SCL3, SPL6, SPL13*, and *MADS-box 25* collectively increased during floral transition (Fig. 5a), suggesting that *DELLA* and

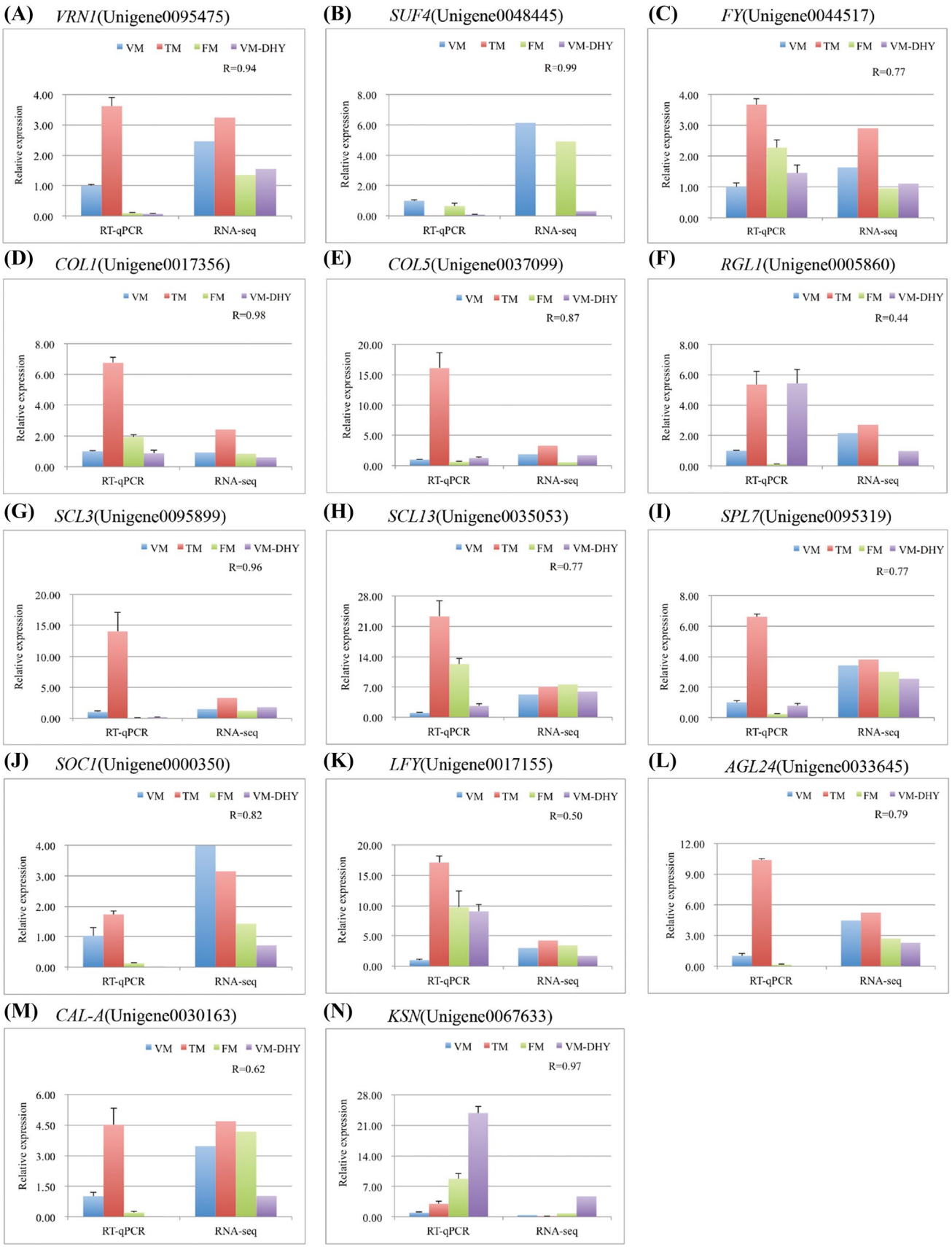
(A) VRN1(Unigene0095475)
VM TM FM VM-DHY
R=0.94
Relative expression
4.00
3.00
2.00
1.00
0.00
RT-qPCR
RNA-seq
(B) SUF4(Unigene0048445)
VM TM FM VM-DHY
R=0.99
Relative expression
8.00
6.00
4.00
2.00
0.00
RT-qPCR
RNA-seq
(C) FY(Unigene0044517)
VM TM FM VM-DHY
R=0.77
Relative expression
4.00
3.00
2.00
1.00
0.00
RT-qPCR
RNA-seq
(D) COL1(Unigene0017356)
VM TM FM VM-DHY
R=0.98
Relative expression
8.00
6.00
4.00
2.00
0.00
RT-qPCR
RNA-seq
(E) COL5(Unigene0037099)
VM TM FM VM-DHY
R=0.87
Relative expression
20.00
15.00
10.00
5.00
0.00
RT-qPCR
RNA-seq
(F) RGL1(Unigene0005860)
VM TM FM VM-DHY
R=0.44
Relative expression
8.00
6.00
4.00
2.00
0.00
RT-qPCR
RNA-seq
(G) SCL3(Unigene0095899)
VM TM FM VM-DHY
R=0.96
Relative expression
20.00
15.00
10.00
5.00
0.00
RT-qPCR
RNA-seq
(H) SCL13(Unigene0035053)
VM TM FM VM-DHY
R=0.77
Relative expression
28.00
21.00
14.00
7.00
0.00
RT-qPCR
RNA-seq
(I) SPL7(Unigene0095319)
VM TM FM VM-DHY
R=0.77
Relative expression
8.00
6.00
4.00
2.00
0.00
RT-qPCR
RNA-seq
(J) SOC1(Unigene0000350)
VM TM FM VM-DHY
R=0.82
Relative expression
4.00
3.00
2.00
1.00
0.00
RT-qPCR
RNA-seq
(K) LFY(Unigene0017155)
VM TM FM VM-DHY
R=0.50
Relative expression
20.00
15.00
10.00
5.00
0.00
RT-qPCR
RNA-seq
(L) AGL24(Unigene0033645)
VM TM FM VM-DHY
R=0.79
Relative expression
12.00
9.00
6.00
3.00
0.00
RT-qPCR
RNA-seq
(M) CAL-A(Unigene0030163)
VM TM FM VM-DHY
R=0.62
Relative expression
6.00
4.50
3.00
1.50
0.00
RT-qPCR
RNA-seq
(N) KSN(Unigene0067633)
VM TM FM VM-DHY
R=0.97
Relative expression
28.00
21.00
14.00
7.00
0.00
RT-qPCR
RNA-seq

◂**Fig. 7** RT-qPCR validation of 14 key candidate floral DEGs in different developmental stages of *R. odorata* var. *gigantea*. The expression levels of genes revealed by RT-qPCR (left side) and RNA-seq (right side). Data from RT-qPCR were means of three replicates and bars represent SE. Data from RNA-seq were means of replicates and were normalized by Log^2 transformed. The correlation coefficient (R) for each gene between RT-qPCR and RNA-seq data was shown and calculated by cor.test in R

SPL are floral activators regulating the rose floral transition. Further experiments are needed to demonstrate their potential functional diversification in the rose flowering compared to flowering in other species.

In contrast to GA, auxin levels and expression of its biosynthetic genes increased from VM to TM, while genes encoding transcriptional repressor proteins, *AUX/IAAs*, had low expression levels (Figs. 1b, 5a). Auxin transport is closely correlated with floral transition, and the dynamic expression of *PIN1* and *LFY* was shown to be synchronous during flowering transition in *A. thaliana* (Heisler et al. 2005). Bai and Demason (2008) reported that auxin and GA could promote the expression of *PIN1* and *LFY*, and an auxin response element was identified in the promoter of *A. thaliana LFY*. Moreover, Yamaguchi et al. (2013) demonstrated a direct positive feedback from *LFY* to the auxin pathway. In this study, *ARF18* and *LFY* had similar expression patterns from VM to TM, whereas *PIN* and *PIN3* expression decreased from VM to TM (Figs. 4b, 5a), indicating that the regulatory function of hormones is different between annuals and perennials. *DELLA* and *YUCCA2* expression correlated well during the rose floral transition (Fig. 6b), suggesting that *DELLA* may mediates the biosynthesis of auxin. Auxin levels peaked at the VM-DHY stage (Fig. 1b), indicating that auxin was not the decisive cue in triggering floral transition. ABA contents and the expression of metabolic genes decreased during floral transition, suggesting that ABA functioned as a repressor of the rose floral transition (Figs. 1b, 5a). Kai et al. (2015) reported that *ABSCISIC ACID-INSENSITIVE* (*ABI4*) repressed floral transition in *A. thaliana* by activating *FLC*. It was also proposed that the regulatory function of ABA in floral transition might converge in a DELLA-dependent manner (Achard et al. 2006).

Sugar signaling regulates flowering transition in rose

Sugars not only function as a source of energy, but act as a florigenic signal in plants (Ortiz-Marchena et al. 2015). It was also reported that *CO* promotes the expression of *GBSS1* (Ortiz-Marchena et al. 2015), and that sugars interacting with age activate *SPL* through *miR156* (Yang et al. 2011). The transformation from vegetative to reproductive growth is mediated by T6P and *SnRK* (Tsai and Gazzarrini 2014). *TPS1* and *SnRK* had an opposite expression pattern during the rose floral transition (Fig. 5a). According the function of sugar and ABA in regulating floral transition in *A. thaliana* (Matsoukas et al. 2013) and the connection of *SnRK* in sugar and ABA signal, we speculated that sugars interact with ABA to mediate the rose floral transition. Starch, in the forms of both amylopectin and amylose, is an important carbon reserve in plants. During floral transition, cellular free sugars are derived from the hydrolysis of linear amylose (Ortiz-Marchena et al. 2015). In *Pyrus pyrifolia*, the activity of sugar catabolizing enzymes was shown to be higher in induced buds than in non-induced buds, suggesting that abundant carbohydrates were consumed in induced buds (Ito et al. 2004). Likewise, the contents of sucrose and starch decreased during floral transition in strawberry (Eshghi and Tafazoli 2015). In this study, comparing the metabolism overview in VM versus TM and VM-DHY versus TM datasets, expression of genes associated with sucrose and starch metabolism, glycolysis and photosynthesis were more intense in the latter (Fig. S6B, C), suggesting the large physiological difference exists between VM and VM-DHY stages. Moreover, the number of up-regulated DEGs associated with starch synthesis and breakdown was more in VM-DHY versus TM than that of VM versus TM. Importantly, the strong correlation was identified between floral genes, *SOC1, AGL24* and starch metabolism genes including *GBSS1, AMY3*, and *BAM3* during floral transition (Fig. 6b). Considering the contents of soluble sugar and starch with negative feedback, we speculated that starch metabolism plays a vast role in mediating the rose floral transition.

The flowering pathway in the rose during floral transition

The seasonal cues of winter cold enable some perennial species to restrict flowering to a short period and then to return to vegetative growth after flowering (Andrés and Coupland 2012). Low temperature inhibits the expression of *FLC*, and activates floral transition in *A. thaliana*, so *FLC* is considered to be a central gene in the vernalization pathway (Ding et al. 2013). In *A. thaliana*, the expression of *FLC* is maintained at a low level in the spring but floral integrators, such as *SOC1* and *FT*, had high expression (Sung and Amasino 2005). In contrast, the inhibition of *PEP1*, which blocks floral transition and facilitates a competence to return to vegetative growth after flowering (Wang et al. 2009), is transient. *KSN* and *FvTFL1*, the homolog of *A. thaliana TFL1*, inhibited the floral transition and had a similar expression pattern in seasonal rose and *Fragaria vesca* (Iwata et al. 2012). In this current study, the expression pattern of *KSN* was similar to the result of previous studies, showing high expression in vegetative buds (Randoux et al. 2014). Randoux et al. also demonstrated that *FT* and *KSN* acted antagonistically with *FD* to induce or inhibit the rose floral transition. However,

the homolog of *FT* was not identified in our study in light of the results of RNA-seq and RT-qPCR, suggesting that there exist other floral activators promoting rose floral transition. Further studies are deeded to elucidate newly floral activators regulating the rose floral transition.

VRN1 is one of several loci that were identified as underlying responses to vernalization, which activates floral transition (Preston and Kellogg 2006) and is induced by low temperatures. It was also reported that *VRN1* was regulated by the circadian clock (Shimada et al. 2009). During the rose floral transition, the expression of *VRN1* increased from VM to TM, and was up-regulated in VM-DHY vs. TM, but was down-regulated in VM versus VM-DHY (Fig. 5a), indicating that *VRN1* is a floral activator in the rose. *VIN3* is especially expressed at low temperatures, and participates in regulation of *FLC* acetylation-levels in the pre-vernalized state, but the inhibition of *FLC* by *VIN3* does not occur when plants are returned to warm temperatures (Sung and Amasino 2004). During the floral transition process, *VIN3* expression level was lower than that of VM-DHY stage (Fig. 5a), suggesting vernalization regulates the expression of *VIN3*.

Rosa odorata var. *gigantea* blooms in early spring. It has been proposed that spring-flowering perennials must undergo a period of exposure to low temperatures to induce floral transition (Gendall et al. 2001). In this study, floral integrator, *AGL24*, showed an increasing expression level from VM to TM, and had low expression level at VM-DHY stage (Fig. 4g). Bielenberg et al. (2008) reported that genes assigned to the *AGL24* clade were characterized as *Dormancy-associated MADS-box* (*DAM*), and were regulated by photoperiod and low temperature in peach (*Prunus persica*) (Li et al. 2009). Based on the time of collecting samples and the results of histological analyses, we identified that floral transition of the rose occurs after bud dormancy. Besides, hormones are known to be involved in bud dormancy release in woody perennials (Horvath et al. 2003). In the study, unigenes associated with the metabolism of several hormones (auxin, GAs, and ABA) differentially expressed between different developmental stages. It seems that the regulatory mechanism of floral transition in woody perennials appears to be more complex than in annuals, and it may be necessary to incorporate the molecular mechanism of bud dormancy in models of the regulatory networks of floral transition.

Together with diurnal change, photoperiod is involved in floral transition. The circadian clock is mediated by phytochromes and cryptochromes (Minni 2005). From our data we infer that *phyA* perceives light signals, including *FHY3* and *FRS*, together with *ELF3*, further controls the circadian clock. We note that *FHY3* represses *CLE*, which controls meristem maintenance, suggesting that light signals participate in the phase change. Additionally, auxin signals indirectly inhibit the expression of *KNOX*, while *KNOX* regulates *GA20ox* and *GA2ox*, reducing the content of GA (Sakamoto et al. 2006), suggesting that hormones modulate the meristem maintenance.

CO plays a central role in photoperiod pathway, which response to circadian clock to induce floral transition (Mouradov et al. 2002). Several *CO-like* genes were identified in this study (Fig. 4e), and showed increasing expression levels during the rose floral transition. Furthermore, *COL1* was closely correlated with *LFY*, and *COL4* with *KNOX, SPL13*, and *MYB* (Fig. 6b), indicating that photoperiod positively regulates the phase transition. Notably, *COL16* had high expression levels at the VM-DHY stage (Fig. 4e), suggesting potential functional diversification.

In summary, the results of this study are valuable for comparative transcriptome analysis between rose species with different flowering behavior, and also provide insights into floral transition in trees. Based on physiological and transcriptomic analyses, we present a model of the regulation of floral transition in *R. odorata* var. *gigantea*. Genes involved in vernalization and photoperiod played crucial roles in inducing flowering, combined with the effects of hormones and starch metabolism.

Acknowledgements Thanks are due to Yuyong Yang (Kunming Yang Chinese Rose Gardening Co., Ltd.) and Haiquan Huang (Southwest Forestry University) for the help and convenience of collecting samples. This work was supported by the Fundamental Research Funds for the Central Universities (No. 2016ZCQ02), National Natural Science Foundation of China (31600565), and Special Fund for Beijing Common Construction Project.

Author contributions ZQX and PHT contributed to the design of the research, GXL collected plant materials, carried out computational analysis and wrote the paper, YC and LL contributed to the design of the research and the manuscript modification. ZN contributed to collect plant materials and plant growing, WHH and LYS contributed to draw graphs, WJ and CTR contributed to modify the manuscript. All authors read and approved the final manuscript.

References

Achard P et al (2006) Integration of plant responses to environmentally activated phytohormonal signals. Science 311:91–94

Andrés F, Coupland G (2012) The genetic basis of flowering responses to seasonal cues. Nat Rev Genet 13:627–639

Bai F, Demason DA (2008) Hormone interactions and regulation of PsPK2: GUS compared with DR5: GUS and PID: GUS in *Arabidopsis thaliana* American. J Bot 95:133–145

Bielenberg DG, Wang Y, Li ZG, Zhebentyayeva T, Fan SH, Reighard GL, Scorza R, Abbott AG (2008) Sequencing and annotation of the evergrowing locus in peach [*Prunus persica* (L.) Batsch] reveals a cluster of six MADS-box transcription factors as candidate genes for regulation of terminal bud formation. Tree Genet Genomes 4:495–507

Blumel M, Dally N, Jung C (2015) Flowering time regulation in crops-what did we learn from Arabidopsis? Curr Opin Biotechnol 32:121–129. https://doi.org/10.1016/j.copbio.2014.11.023

Böhlenius H, Huang T, Charbonnelcampaa L, Brunner AM, Jansson S, Strauss SH, Nilsson O (2006) CO/FT regulatory module controls timing of flowering and seasonal growth cessation in trees. Science 312:1040–1043

Boss PK, Thomas MR (2002) Association of dwarfism and floral induction with a grape 'green revolution' mutation. Nature 416:847–850

Bouché F, D'Aloia M, Tocquin P, Lobet G, Detry N, Périlleux C (2016) Integrating roots into a whole plant network of flowering time genes in *Arabidopsis thaliana*. Sci Rep 6:203–214

Cutler SR, Rodriguez PL, Finkelstein RR, Abrams SR (2010) Abscisic acid: emergence of a core signaling network. Annu Rev Plant Biol 61:651–679

Ding L, Kim SY, Sd M (2013) FLOWERING LOCUS C EXPRESSOR family proteins regulate FLOWERING LOCUS C expression in both winter-annual and rapid-cycling Arabidopsis. Plant Physiol 163:243–252

Dubois A et al. (2011) Genomic approach to study floral development genes in *Rosa* sp. PLoS ONE 6:e28455 https://doi.org/10.1371/journal.pone.0028455

Eshghi S, Tafazoli E (2015) Possible role of non-structural carbohydrates in flower induction in strawberry. J Hortic Sci Biotechnol 81:854–858

Fan Z, Li J, Li X, Wu B, Wang J, Liu Z, Yin H (2015) Genome-wide transcriptome profiling provides insights into floral bud development of summer-flowering *Camellia azalea*. Sci Rep 5:9729

Fornara F, de Montaigu A, Coupland G (2010) SnapShot: control of flowering in Arabidopsis. Cell. https://doi.org/10.1016/j.cell.2010.04.024

Foster T, Johnston R, Seleznyova A (2003) A morphological and quantitative characterization of early floral development in apple (malus × domestica borkh.). Ann Bot 92:199–206

Fu J, Wang L, Yi W, Yang L, Yang Y, Dai S (2014) Photoperiodic control of FT- like gene ClFT initiates flowering in *Chrysanthemum lavandulifolium*. Plant Physiol. Biochem. 74:230–238

Gendall AR, Levy YY, Wilson A, Dean C (2001) The VERNALIZATION 2 gene mediates the epigenetic regulation of vernalization in Arabidopsis. Cell 107:525–535

Grabherr MG et al (2011) Full-length transcriptome assembly from RNA-Seq data without a reference genome. Nat Biotechnol 29:644–652

Hararisteinberg O, Ohad I, Chamovitz DA (2001) Dissection of the light signal transduction pathways regulating the two early light-induced protein genes in Arabidopsis. Plant Physiol 127:986–997

He ZF (1985) The fast determination method for content of glucose, frutose by anthrone colorimetry. In: He ZF (ed) Grain quality and it's analysis technology, Agricultural Press, Beijing, pp 144–150

Hedden P, Thomas SG (2012) Gibberellin biosynthesis and its regulation. Biochem J 444:11–25

Heisler MG, Ohno C, Das P, Sieber P, Reddy GV, Long JA, Meyerowitz EM (2005) Patterns of auxin transport and gene expression during primordium development revealed by live imaging of the Arabidopsis inflorescence meristem. Curr Biol 15:1899–1911

Horibe T, Yamada K, Otagaki S, Matsumoto S, Kawamura K (2013) Molecular genetic studies on continuous-flowering roses that do not originate from *Rosa chinensis*. Acta Hortic 2013:1064

Horvath DP, Anderson JV, Chao WS, Foley ME (2003) Knowing when to grow: signals regulating bud dormancy. Trends Plant Sci 8:534–540

Ito A, Hayama H, Kashimura Y (2004) Possible roles of sugar concentration and its metabolism in the regulation of flower bud formation in Japanese Pear (*Pyrus pyrifolia*). Acta Hortic 636:365–373

Iwata H et al (2012) The TFL1 homologue KSN is a regulator of continuous flowering in rose and strawberry. Plant J 69:116–125. https://doi.org/10.1111/j.1365-313X.2011.04776.x

Jin J et al (2015) An arabidopsis transcriptional regulatory map reveals distinct functional and evolutionary features of novel transcription factors. Mol Biol Evol 32:1767–1773

Kai S et al (2015) ABSCISIC ACID-INSENSITIVE 4 negatively regulates flowering through directly promoting Arabidopsis FLOWERING LOCUS C transcription. J Exp Bot 67:195–205

Kang C, Darwish O, Geretz A, Shahan R, Alkharouf N, Liu Z (2013) Genome-scale transcriptomic insights into early-stage fruit development in woodland strawberry *Fragaria vesca*. Plant Cell 25:1960–1978

Kawamura K, Oyant HS, Thouroude T, Jeauffre J, Foucher F (2015) Inheritance of garden rose architecture and its association with flowering behaviour. Tree Genet Genomes 11:1–12

Khan MRG, Ai XY, Zhang JZ (2014) Genetic regulation of flowering time in annual and perennial plants. Wiley Interdisc Rev 5:347–359

Kim DH, Doyle MR, Sung SB, Amasino RM (2009) Vernalization: winter and the timing of flowering in plants. Annu Rev Cell Dev Biol 25:277–299

Kinmonth-Schultz HA, Tong X, Lee J, Song YH, Ito S, Kim SH, Imaizumi T (2016) Cool night-time temperatures induce the expression of CONSTANS and FLOWERING LOCUS T to regulate flowering in Arabidopsis. New Phytol. https://doi.org/10.1111/nph.13883

Kotoda N, Iwanami H, Takahashi S, Abe K (2006) Antisense expression of MdTFL1, a TFL1-like gene, reduces the juvenile phase in apple. J Am Soc Hortic Sci 131:74–81

Lastdrager J, Smeekens S (2014) Sugar signals and the control of plant growth and development. J Exp Bot 65:799–807

Lenhard M, Bohnert A, Jurgens G, Laux T (2001) Termination of stem cell maintenance in Arabidopsis floral meristems by interactions between WUSCHEL and AGAMOUS. Cell 105:805–814

Li Z, Reighard GL, Abbott AG, Bielenberg DG (2009) Dormancy-associated MADS genes from the EVG locus of peach [*Prunus persica* (L.) Batsch] have distinct seasonal and photoperiodic expression patterns. J Exp Bot 60:3521–3530

Lohse M et al (2014) Mercator: a fast and simple web server for genome scale functional annotation of plant sequence data. Plant Cell Environ 37:1250–1258. https://doi.org/10.1111/pce.12231

Matsoukas IG, Massiah AJ, Thomas B (2013) Starch metabolism and antiflorigenic signals modulate the juvenile-to-adult phase transition in Arabidopsis. Plant Cell Environ 36:1802–1811

Minni (2005) Integration of light signaling with photo periodic flower in gand circadian rhythm. Cell Res 15:559–566

Moriya Y, Itoh M, Okuda S, Yoshizawa AC, Kanehisa M (2007) KAAS: an automatic genome annotation and pathway reconstruction server. Nucleic Acids Res 35:W182–W185

Mortazavi A, Williams BA, McCue K, Schaeffer L, Wold B (2008) Mapping and quantifying mammalian transcriptomes by RNA-Seq. Nat Methods 5:621–628

Mouradov A, Cremer F, Coupland G (2002) Control of flowering time: interacting pathways as a basis for diversity. Plant cell 14:S111–S130

Nishikawa F, Endo T, Shimada T, Fujii H, Shimizu T, Omura M, Ikoma Y (2007) Increased CiFT abundance in the stem correlates with floral induction by low temperature in Satsuma mandarin (*Citrus unshiu* Marc.). J Exp Bot 58:3915–3927

Nishikawa F, Endo T, Shimada T, Fujii H, Shimizu T, Omura M (2009) Differences in seasonal expression of flowering genes between deciduous trifoliate orange and evergreen *Satsuma mandarin*. Tree Physiol 29:921–926

Ortiz-Marchena MI, Romero JM, Valverde F (2015) Photoperiodic control of sugar release during the floral transition: what is the role of sugars in the florigenic signal? Plant Signal Behav 10:e1017168. https://doi.org/10.1080/15592324.2015.1017168

Pan X, Welti R, Wang X (2010) Quantitative analysis of major plant hormones in crude plant extracts by high-performance liquid chromatography–mass spectrometry. Nat Protoc 5:986–992

Preston JC, Kellogg EA (2006) Reconstructing the evolutionary history of paralogous APETALA1/FRUITFULL-like genes in grasses (Poaceae). Genetics 174:421–437

Randoux M et al (2012) Gibberellins regulate the transcription of the continuous flowering regulator, RoKSN, a rose TFL1 homologue. J Exp Bot. https://doi.org/10.1093/jxb/errs3130

Randoux M et al (2014) RoKSN, a floral repressor, forms protein complexes with RoFD and RoFT to regulate vegetative and reproductive development in rose. New Phytol 202:161–173. https://doi.org/10.1111/nph.12625

Sakamoto T et al (2006) Ectopic expression of KNOTTED1-like homeobox protein induces expression of cytokinin biosynthesis genes in rice. Plant Physiol 142:54–62

Schmittgen TD, Livak KJ (2008) Analyzing real-time PCR data by the comparative CT method. Nat Protoc 3:1101–1108

Shimada S et al (2009) A genetic network of flowering-time genes in wheat leaves, in which an APETALA1/FRUITFULL-like gene, VRN1, is upstream of FLOWERING LOCUS T. Plant J 58:668–681. https://doi.org/10.1111/j.1365-313X.2009.03806.x

Sung S, Amasino RM (2004) Vernalization in *Arabidopsis thaliana* is mediated by the PHD finger protein VIN. Nature 427(3):159–164

Sung S, Amasino RM (2005) Remembering winter: toward a molecular understanding of vernalization. Annu Rev Plant Biol 56:491–508

Supek F, Bosnjak M, Skunca N, Smuc T (2011) REVIGO summarizes and visualizes long lists of gene ontology terms. PLoS ONE 6:e21800. https://doi.org/10.1371/journal.pone.0021800

Thissen D, Kuang D (2010) Quick and easy implementation of the Benjamini-Hochberg procedure for controlling the false positive rate in multiple comparisons. J Educ Behav Stat 27:77–83

Tsai AYL, Gazzarrini S (2014) Trehalose-6-phosphate and SnRK1 kinases in plant development and signaling: the emerging picture. Front Plant Sci 5:119–119

Usadel B, Poree F, Nagel A, Lohse M, Czedik-Eysenberg A, Stitt M (2009) A guide to using MapMan to visualize and compare Omics data in plants: a case study in the crop species, maize. Plant Cell Environ 32:1211–1229

Wang R et al (2009) PEP1 regulates perennial flowering in *Arabis alpina*. Nature 459:423–427

Wang F, Lian LJ, Liu QL (2015) Low expression of RTFL1c releases expression of RLFY, which induces recurrent flowering in rose. Acta Hortic 1064:131–134

Wolfe CJ, Kohane IS, Butte AJ (2005) Systematic survey reveals general applicability of "guilt-by-association" within gene coexpression networks. BMC Bioinform 6:227

Yamaguchi N et al (2013) A molecular framework for auxin-mediated initiation of flower primordia. Dev Cell 24:271–282. https://doi.org/10.1016/j.devcel.2012.12.017

Yamaguchi N, Winter CM, Wu MF, Kanno Y, Yamaguchi A, Seo M, Wagner D (2014) Gibberellin acts positively then negatively to control onset of flower formation in Arabidopsis. Science 344:638–641

Yang L, Conway SR, Poethig RS (2011) Vegetative phase change is mediated by a leaf-derived signal that represses the transcription of miR. Development 138(2):245–249

Young MD, Wakefield MJ, Smyth GK, Oshlack A (2010) Gene ontology analysis for RNA-seq: accounting for selection bias. Genome Biol 11:1

Yu JW et al (2009) COP1 and ELF3 control circadian function and photoperiodic flowering by regulating GI stability. Mol Cell 32:617–630

Yu S et al (2012) Gibberellin regulates the Arabidopsis floral transition through miR156-targeted SQUAMOSA PROMOTER BINDING–LIKE transcription factors. Plant Cell 24:3320–3332

Zhang ZL et al (2011) SCARECROW-LIKE 3 promotes gibberellin signaling by antagonizing master growth repressor DELLA in Arabidopsis. Proc Natl Acad Sci USA 108:2160–2165

Zhao Y, Medrano L, Ohashi K, Fletcher JC, Yu H, Sakai H, Meyerowitz EM (2004) HANABA TARANU is a GATA transcription factor that regulates shoot apical meristem and flower development in Arabidopsis. Plant Cell 16:2586–2600